AGU PUBLICATIONS

GeoHealth

RESEARCH ARTICLE
10.1002/2017GH000059

Key Points:
- High PM_{10} is observed during haze period of February to April in Northern Thailand when intensive forest fires and stagnant air are prevalent
- Incorporation of synoptic meteorology patterns, classified by an automated scheme, could improve AOT-PM_{10} regression model
- Spatially continuous MODIS AOT values were used for haze exposure mapping and illustrated by a case study for Chiangmai province

Supporting Information:
- Supporting Information S1

Correspondence to:
N. T. Kim Oanh,
kimoanh@ait.ac.th

Citation:
Leelasakultum, K., and N. T. Kim Oanh (2017), Mapping exposure to particulate pollution during severe haze episode using improved MODIS AOT-PM_{10} regression model with synoptic meteorology classification, *GeoHealth*, *1*, 165–179, doi:10.1002/2017GH000059.

Received 29 JAN 2017
Accepted 18 MAY 2017
Accepted article online 23 MAY 2017
Published online 14 JUN 2017

Mapping exposure to particulate pollution during severe haze episode using improved MODIS AOT-PM_{10} regression model with synoptic meteorology classification

Ketsiri Leelasakultum[1] and Nguyen Thi Kim Oanh[1]

[1]Environmental Engineering and Management, Asian Institute of Technology, Pathumthani, Thailand

Abstract Severe smoke haze from biomass burning is frequently observed in Northern Thailand during dry months of February–April. Sparsely located monitoring stations operated in this vast mountainous region could not provide sufficient particulate matter (PM) data for exposure risk assessment. Satellite aerosol optical thickness (AOT) data could be used, but their reliable relationship with ground-based PM data should be first established. This study aimed to improve the regression model between PM_{10} and Moderate Resolution Imaging Spectroradiometer AOT with consideration of synoptic patterns to better assess the exposure risk in the area. Among four synoptic patterns, each representing the totality of meteorology governing Northern Thailand on a given day, most severe haze days belonged to pattern 2 that featured conditions of clear sky, stagnant air, and high PM_{10} levels. AOT-24 h PM_{10} regression model for pattern 2 had coefficient of determination improved to 0.51 from 0.39 of combined case. Daily exposure maps to PM_{10} in most severe haze period of February–April 2007 were produced for Chiangmai, the largest and most populated province in Northern Thailand. Regression model for pattern 2 was used to convert 24 h PM_{10} ranges of modified risk scale to corresponding AOT ranges, and the mapping was done using spatially continuous AOT values. The highest exposure risk to PM_{10} was shown in urban populated areas. Larger numbers of forest fire hot spots and more calm winds were observed on the days of higher exposure risk. Early warning and adequate health care plan are necessary to reduce exposure risk to future haze episodes in the area.

1. Introduction

In Asian developing countries, intensive emissions from numerous sources, such as biomass open burning, industry, traffic, and residential combustion, cause alarmingly high air pollution levels with consequent harmful effects to the local environment and regional climate [*World Health Organization (WHO)*, 2014; *United Nation Environment Program-World Meteorological Organization*, 2011]. Specifically, the levels of particulate matter (PM) air pollution have been reported to be high in many locations in Asia [*Kim Oanh et al.*, 2006; *Hopke et al.*, 2008], hence making this pollutant the most concerned from the health effects point of view. Atmospheric PM, a complex mixture of particles and droplets that are suspended in the air, is characterized by diverse size, composition, and emission sources/origins. PM is commonly classified based on their size because of the associated difference in health effects. Total suspended PM (TSP) includes particles of all sizes, ranging from the smallest particles to the largest suspended particles (normally with the cutoff aerodynamic diameter in between 25 and 50 μm) that are sampled by a high-volume sampler. PM_{10} is a subset of TSP that composes of all particles having the aerodynamic diameters not above 10 μm. These particles can enter the human respiratory track, or they are respirable. PM_{10} is commonly divided into the fine particle fraction or $PM_{2.5}$ (particles with aerodynamic diameters not above 2.5 μm) and coarse PM fraction or $PM_{10-2.5}$. These two fractions of PM_{10} have different sources/origins, composition, and different potential effects on health and environment. $PM_{2.5}$ consists of both primary particles that are directly emitted from the combustion sources and the secondary particles that are formed in the atmosphere as a result of complex photochemical reactions involving precursor gases of nitrogen oxides and oxides of sulfur, ammonia, and volatile organic compounds [*WHO*, 2003]. The coarse PM is mainly of geological origin but may also contain sea salt, bioaerosol (pollens, spores, plant parts, etc.), and particles from uncontrolled combustion emissions [*Watson and Chow*, 2002].

The fine particles of $PM_{2.5}$ have the potential to penetrate deeper into the respiratory system, hence causing more risk to the human health than the coarse PM fraction [*Fann et al.*, 2012; *Tillett*, 2012]. Overall, exposure to

high concentrations of PM_{10} (both fine and coarse fractions) has been reported to show strong association with mortality [*Park et al.*, 2013; *Zhou et al.*, 2013], respiratory symptoms, brain function deficiency such as cognitive decline [*Weuve et al.*, 2012], sleeping pattern disturbances in children [*Abou-Khadra*, 2013], and even the adverse birth outcomes [*Sapkota et al.*, 2012]. *Ostro et al.* [1999] reported for Bangkok City that a 10 $\mu g\ m^{-3}$ increment in the daily PM_{10} concentration was associated with 1–2% increase in the daily natural mortality, 1–2% increase in cardiovascular mortality, and a 3–6% increase in respiratory mortality. *Brunekreef and Forsberg* [2005] argued that due to their distinct sources and consequently the composition, the health impact of the coarse ($PM_{2.5-10}$) and fine fractions ($PM_{2.5}$) needs to be studied separately. They also found some correlation between coarse fraction concentrations and cardiovascular hospitalizations, whereas $PM_{2.5}$ was more strongly correlated with overall mortality than coarse fraction.

There are growing efforts to monitor ambient PM in many countries. Majority of the routine PM measurements in the developing countries are still focusing on PM_{10}, mainly due to the lack of facilities for monitoring of $PM_{2.5}$ [*Kim Oanh et al.*, 2012] or finer PM such as ultrafine particles. The information on PM levels is still largely insufficient and generally has a limited spatial coverage because most air pollution monitoring efforts are concentrated in urban areas [*Kim Oanh et al.*, 2012, and references therein]. For example, the information of $PM_{2.5}$ in developing Asian countries is still fragmented and mainly generated by international research projects [*Kim Oanh et al.*, 2006; *Hopke et al.*, 2008]. Much less information of PM pollution has been found for rural and remote areas, although pollution levels in the remote areas may be high [*Co et al.*, 2014; *Kim Oanh et al.*, 2016], especially during episodic biomass burning events [*Kim Oanh and Leelasakultum*, 2011]. The limited spatial coverage of the PM monitoring data can reduce the statistical strength of the relationships between pollutant levels and health effects that are essential for exposure assessment studies [*Liu et al.*, 2009].

Satellite remote sensing is a tool for PM monitoring that has been evaluated and used in a number studies, especially in places where ground measurements are limited. Satellite data have a large spatial coverage and relatively long term series [*Engel-Cox et al.*, 2013; *Lee et al.*, 2011; *Engel-Cox et al.*, 2004; *Gupta and Christopher*, 2008], hence can provide suitable information for exposure assessment, especially for the large-scale studies [*van Donkelaar et al.*, 2016]. The satellite aerosol optical thickness (AOT), which is the extinction of radiation caused by aerosol in the atmospheric column under observation, is the principal data product used for assessment of the PM pollution. AOT characterizes the total amount of particles in the vertical column above a grid/area of the Earth surface. The ground-based PM data, produced at a monitoring station, instead represent the pollution levels measured at a single point located at few meters aboveground. Due to this mismatch, the use of AOT to estimate ground-based PM levels is not always straightforward. In addition, ground-based PM data are time averaged, normally hourly or 24 hourly, while AOT is a snapshot produced at the passing time of a satellite over a location. Both AOT and ground-based PM data contain measurement uncertainties that largely depend on environmental conditions, such as meteorology, or presence of emission sources in vicinity of ground-based monitors; hence, simple relationships may not always provide satisfactory estimates. A simple linear regression analysis is commonly used in studies conducted to estimate PM based on AOT products [e.g., *Wang and Christopher*, 2003; *Engel-Cox et al.*, 2004], but several more recent studies also relied on more complex models, e.g., *Lee et al.* [2011], *Tsai et al.* [2011], *Liu et al.* [2009], and *Chudnovsky et al.* [2014]. These complex regression models between AOT and PM were generally developed with inclusion of other parameters, such as local meteorology (temporal predictors) and land use information (spatial predictors). The inclusion of the temporal and spatial variables as covariates in the regression has been reported to improve the models for predicting ground-based $PM_{2.5}$ from AOT values [*Liu et al.*, 2005, 2007, 2009; *Chudnovsky et al.*, 2014].

Specifically, meteorological parameters, e.g., relative humidity, planetary boundary layer, and wind (speed and direction), have been shown to affect the correlations (R) between AOT and ground-based PM measurements [*Liu et al.*, 2005; *Chudnovsky et al.*, 2014]. Some of the meteorological variables, for example, relative humidity, can affect the particle size as well as the extinction of radiation in the atmosphere [*Malm et al.*, 2000]. In reality, the meteorological variables are interrelated; hence, instead of investigation of the effects of individual meteorological variable/predictor on the regression model to estimate PM from AOT data, an alternative way is to consider the totality of meteorological variables associated with different air mass types or synoptic patterns. *Yahi et al.* [2013] reported improvement of the AOT (ground-based) and PM_{10} (particles with aerodynamic diameter not above 10 μm) with consideration of the weather types that were classified

using tridimensional mesoscale wind and temperature. *Zeeshan and Kim Oanh* [2014] applied an automated synoptic climatological classification scheme to identify the synoptic pattern governing, on a given day, the type and development tendency of the air mass over the central part of Thailand. The study found noticeable increase in correlations (between AOT and PM_{10}) in those patterns that have high PM levels and shallow mixing layers when most of the aerosol appeared near the ground (as seen from the backscatter coefficients). Previous studies that aimed to predict PM levels using Moderate Resolution Imaging Spectroradiometer (MODIS) AOT data in developed countries had focused more on $PM_{2.5}$ than PM_{10} (Table S1 in the supporting information) perhaps due to the availability of the ground monitoring data [*Zhang et al.*, 2009; *Engel-Cox et al.*, 2004; *Liu et al.*, 2007, 2009; *Chudnovsky et al.*, 2014, and references therein]. Most of the studies in the developing countries were, however, still focusing on PM_{10}, and the results confirmed a linear relationship between AOT and PM_{10} but with a wide range of the coefficient of determination (R^2) or correlation (Table S1 and further detailed in *Song et al.* [2009], *Yahi et al.* [2013], *Zheng et al.* [2013], *Yap and Hashim* [2013], *Zeeshan and Kim Oanh* [2014], and *Li et al.* [2015]). The coarse fraction ($PM_{10-2.5}$) of PM_{10} can gravitationally deposit to surfaces, hence limiting their atmospheric lifetime to a few hours after emissions, and this makes them less homogeneously distributed over a geographical location. $PM_{2.5}$, the fine fraction of PM_{10}, can remain suspended for several days to weeks, depending mainly on meteorological conditions; hence, they tend to be more homogeneously distributed with distance from the emission source [*Watson and Chow*, 2002]. In addition, the secondary particles constituting a large part of $PM_{2.5}$ in forms of sulfates, nitrates, and organic particles are well distributed as they are the results of formation processes of regional scales. The fact that the coarse particles are more locally distributed near their emission sources would potentially cause a larger uncertainty in the regression between point-based ground level measurements and spatially averaged AOT data. This may be a reason for lower correlations found between AOT-PM_{10} than AOT-$PM_{2.5}$ in several cases (*Guo et al.* [2010], *Zeeshan and Kim Oanh* [2014], and others listed in Table S1).

The ratio between the fine and coarse fractions ($PM_{2.5}/PM_{10}$), however, depends on the season and the location of the monitoring sites [*Kim Oanh et al.*, 2006]. Biomass open burning emissions have a small coarse PM fraction; hence, PM_{10} and $PM_{2.5}$ concentrations in the smoke are quite close [*Kim Oanh et al.*, 2010]. Remote areas in Southeast Asia normally tend to have higher ratios of $PM_{2.5}/PM_{10}$ (0.70–0.80), especially in the dry season, because of the dominant contribution from biomass open burning and secondary particles mainly in the fine fraction [*Co et al.*, 2014; *Kim Oanh et al.*, 2016].

Northern Thailand, a mountainous region vastly covered by natural forests, shares the border to Myanmar and Laos. The region has experienced severe haze episodes during dry and hot months, February–April, every year. Open biomass burning, especially the forest fires in Thailand and the neighboring countries, was identified as the main cause of the haze [*Kim Oanh and Leelasakultum*, 2011; *Sukitpaneenit and Kim Oanh*, 2014]. The high PM pollution levels observed during the haze periods raise a public concern on health effects. There has yet a comprehensive assessment of the PM exposure risk for people living in the region during haze events, and this is partly due to the lack of air pollution monitoring data. The monitoring data generated by the sparsely distributed automatic monitoring stations, only five stations over the domain (Figure S1 in the supporting information), operated by the Pollution Control Department (PCD) of Thailand could not provide the necessary spatial coverage for a comprehensive exposure assessment. The records of inpatients and outpatients are normally available at a few large hospitals and may not represent the risk of exposure of all people in every commune of a province, especially those living in more remote areas. In addition, it is always difficult to separate the patients suffering from respiratory diseases caused by the exposure to the haze pollution, for example, from those who got the diseases due to other causes [*Chiangmai Provincial Public Health Office (CMPHO)*, 2008]. A haze pollution metric that has a better spatial coverage such as satellite AOT would be very useful in this case [*Lee et al.*, 2011].

The main aim of this study was to improve the regression model between PM_{10} and satellite AOT to better assess the exposure risk in Northern Thailand during the haze prone periods. Our previous work [*Kim Oanh and Leelasakultum*, 2011] has developed an automated scheme, using a statistical pattern recognition technique, to classify the governing meteorological conditions over Northern Thailand into four synoptic patterns. Each pattern has been found to associate with a specific PM pollution range. As a follow-up step, in the current study, we examined possible improvement of the regression models between AOT and PM_{10} (there was no systematic $PM_{2.5}$ data available for the purpose) when the synoptic patterns were considered for the

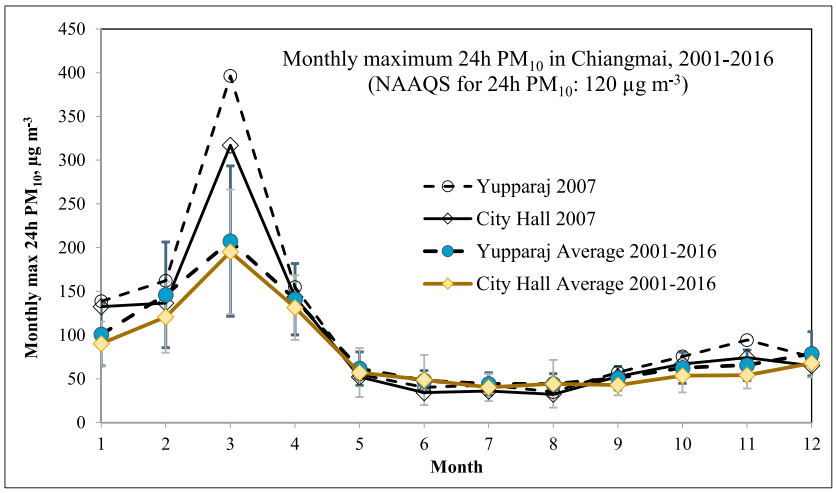

Figure 1. Monthly maximum 24 h PM_{10} measured at two sites in Chiangmai in 2007 as compared to the average for 2001–2016 (based on raw data of *PCD* [2017]).

most severe haze period in the past 16 years (2001–2016). Subsequently, to illustrate the approach, the daily exposure maps to PM_{10} pollution for the most haze-prone pattern (pattern 2) were developed based on satellite AOT data with the aid of the geographic information system (GIS) for the Chiangmai province, the largest and most populated province in Northern Thailand.

2. Methodology

2.1. Study Area

The northern region of Thailand (Northern Thailand) has an area of 93,690 km^2 that is mostly covered by forest, while agricultural activities and residential areas shared only about 30% of the total area. The climate of Northern Thailand is influenced by the tropical monsoons. The southwest monsoon produces wet weather and normally starts in mid-May and lasts until mid-October. The northeast monsoon is usually prevalent from mid-October to mid-February and produces relatively cold and dry weather over the region. The period from mid-February until mid-May can be defined as a transitional period with the hottest weather observed in March–April; hence, it is also known as the local summer. During this local summer period, most forest fire events are reported [*Sukitpaneenit and Kim Oanh*, 2014].

To develop the relationship between the satellite AOT and ground-based PM monitoring data (AOT-PM), we considered the monitoring data collected from automatic monitoring stations in five provinces in Northern Thailand (Chiang Mai, Chiang Rai, Lampang, Maehongson, and Nan provinces) with the locations given in Figure S1. These five provinces collectively had an area of 61,504 km^2 and population of 4,275,006 [*National Statistical Office of Thailand (NSO)*, 2016]. Chiangmai is the largest (20,107 km^2) and most populated (over 1,737,000) province in the domain with its capital city, the Chiangmai City, being the second largest in Thailand after Bangkok. The Chiangmai province has a large forest coverage (Figure S2). Forest fires often occur in the province during the dry period from February to April [*Forest Fire Control Division*, 2011] and cause high air pollution levels [*Kim Oanh and Leelasakultum*, 2011]. Figure 1 shows the high average of the monthly maximum 24 h PM_{10} (the highest 24 h value per month) observed consistently during the dry months recorded at two automatic monitoring stations in Chiangmai in the last 16 years (2001–2016). The most severe haze episode was observed in March 2007 when daily (24 h) PM_{10} reached the peaks of 317 and 396 µg m^{-3}, respectively, at two stations, i.e., well above the 16 year (2001–2016) average for March of about 200 µg m^{-3}. The hospital records also showed a sharp increase in the number of respiratory patients in March 2007 as compared to the same month in other precedent years [*CMPHO*, 2008]. This study, therefore, conducted mapping of exposure risk during this severe haze period, February to April of 2007, for the Chiangmai province.

2.2. Data Collection and Analysis

The PM_{10} concentrations were collected from February to April 2007 from five PCD monitoring stations that had the data during the study period: two stations in Chiangmai, one station in Chiangrai, one station in Lampang, and one station in Mae Hong Son (Figure S1). Two stations in Chiangmai (Chiangmai City Hall and Yupparaj) and the station in Lampang (Lampang City Hall station) used the Tapered-Element Oscillating Microbalance instruments for hourly PM_{10} recording, while the stations in Chiangrai and Mae Hong Son used the beta attenuation method (beta gauge). These two equivalent methods are specified in the Thailand Ambient Air Standards, and they have been assessed for the data comparability [*Pollution Control Department (PCD)*, 2017]. The QA/QC procedure applied for the PCD stations is well established (http://infofile.pcd.go.th/air/).

This study used the AOT product of Moderate Resolution Imaging Spectroradiometer (MODIS) on board of Terra and Aqua satellites, downloaded from the NASA website (http://ladsweb.nascom.nasa.gov). The AOT data were the processed data MOD04 and MYD04 of variables "Optical_Depth_Land_And_Ocean," which are level 2 products of Terra and Aqua satellites, respectively. The MODIS product has a spatial resolution of 10×10 km^2, and the measurement times are approximately at 10:30 A.M. and 1:30 P.M. local standard time (LST) for any location on Earth according to the passing time of the satellites [*Engel-Cox et al.*, 2006]. The MODIS AOT data were downloaded for the study domain of 17–21°N and 97–100°E, 2 times per day (Terra AOT and Aqua AOT) for every day in the period from 1 February to 30 April 2007, i.e., the same period as the ground monitoring PM_{10} data.

One pixel of MODIS AOT covers an area of 10×10 km^2; hence, to match the data spatially, the search radius for the AOT retrieval was set at 0.05° (about 6 km) from the respective ground station location [*Sohrabinia and Khorshiddoust*, 2007]. Temporally, we tried both hourly (1 h) and 24 h PM_{10} to match with each and both Terra AOT and Aqua AOT values of the day. The 24 h PM_{10}, as shown later, showed a better correlation with MODIS AOT data than hourly PM_{10}. Besides, 24 h PM_{10} is considered as more relevant for the exposure assessment than the values measured with shorter averaging time such as hourly or 2 hourly.

As the satellite MODIS AOT is measured from the space, it is generally recommended that the data should be validated using the ground-based AOT produced by the Sun photometer. This study used the Sun photometer data (level 2 quality controlled) measured at the Chiangmai site (18.81°N; 98.99°E) downloaded from the Aerosol Robotic Network (AERONET) website for the purpose. The Sun photometer data for Chiangmai, here called AERONET AOT, were only available for 12 days, mainly in April 2007, during the study period; hence, only a small set of data was available for the validation of the MODIS AOT. Note that the AERONET AOT was recorded at several wavelengths, ranging from 0.34 μm to 1.6 μm, but none is the same as any wavelength of MODIS AOT. Therefore, the quadratic interpolation method [*O'Neill et al.*, 2003] was used to calculate the AERONET AOT at 0.55 μm from the data of all provided wavelengths. Further, we used the AERONET AOT observed during the time period of 10:30 ± 15 and 13:30 ± 15 to compare with the Terra and Aqua AOT, respectively [*Hyer et al.*, 2011]. The results showed a good linear relationship with R^2 of 0.93, but AERONET AOT values were consistently higher than the MODIS AOT with a regression line slope of 0.76 (Figure S3). In a previous study [*Zeeshan and Kim Oanh*, 2014], the regression of MODIS AOT versus AERONET AOT for the central part of Thailand using a much bigger data set (2 times daily for over 5 years) had a larger slope of the regression line (0.91) but lower R^2 (0.81).

2.3. Effects of Synoptic Patterns on AOT-PM_{10} Relationships

2.3.1. Synoptic Pattern Clarification

The meteorology conditions (synoptic weather situations) governing over Northern Thailand had been classified into four homogenous patterns in our previous study [*Kim Oanh and Leelasakultum*, 2011] using an automated meteorology classification scheme developed thereby for the purpose. The classification was done using the surface meteorological data at 7:00 LST (00:00 UTC) in February-March-April months of 8 years (2001–2008) from the regional meteorology stations: four stations in Thailand (Chiangmai, Bangkok, Nongkhai, and Nakhonpanom) and three stations in China (Yibin, Wuhan, and Haikou). The morning mixing height in Chiangmai, determined by the air parcel method, was also included. More information on the 18 meteorological variables included in the final data set used for the meteorology classification, extracted from *Kim Oanh and Leelasakultum* [2011], is given in Textbox S1 in the supporting information.

The principal component analysis was applied to the correlation matrix of the standardized meteorological variables. The Varimax rotation was performed so that each principal component would represent maximum possible variance in the original data set. The resulting component scores were then segregated to produce meteorologically homogeneous categories using a two-stage clustering approach, the hierarchical clustering (average linkage) followed by the *k*-means clustering technique [*Steinbach et al.*, 2000]. The classification of synoptic patterns using this automated scheme is expected to have more objectivity as compared to the classification by using visual comparison of synoptic charts, for example.

The average meteorological characteristics observed at Chiangmai and Bangkok meteorology stations in the four synoptic patterns are presented in Table S2. The detailed description and the synoptic charts of each pattern are provided in our previous study [*Kim Oanh and Leelasakultum*, 2011]. As a way of examples, the synoptic charts of days belonging to different patterns are given in Figure S4. Briefly, pattern 1 has the highest average cloudiness (6/10), mixing height, dew point, and visibility and the second highest values of sea level pressure and wind speed (1.1 m s^{-1}). Pattern 2 is characterized by a clear sky with the lowest cloudiness (1/10), lowest mixing height, lowest sea level pressure (due to a presence of several thermal lows over Northern Thailand that induced hot weather in the study area), and the second lowest wind speed (average of 0.2 m s^{-1}) and dew point. Pattern 3 is characterized by the highest wind speed (1.9 m s^{-1}), the second highest values of mixing height, dew point, and visibility, with relatively clear sky conditions (cloudiness: 2.4/10). Pattern 4 also shows relatively clear sky conditions (cloudiness: 2/10), the weakest wind (0.1 m s^{-1}), and the highest sea level pressure (with a strong high-pressure ridge observed over Northern Thailand in synoptic charts). Note that pattern 2 was the most prevalent pattern during the study period when haze episodes were recorded.

Zeeshan and Kim Oanh [2014] improved the correlation (*R*) between AOT and PM_{10} time series for the central part of Thailand by incorporating synoptic patterns. Specifically, the study produced higher *R* values (than the lump sum case) for two synoptic patterns that were characterized by high PM_{10} and shallower mixing layers. Therefore, in the present study, we also analyzed the AOT and PM_{10} relationships with considerations of the synoptic patterns to produce improved regression models for use in the PM exposure mapping.

2.4. Mapping Exposure Risk to PM_{10} for Chiangmai Province

The risk levels of 24 h PM_{10} exposure were classified by incorporating the Air Quality Index (AQI) scales of Thailand [*PCD*, 2017] and U.S. Environmental Protection Agency (https://airnow.gov/index.cfm?action=pubs.aqguidepart). Accordingly to *PCD* [2017], if 24 h PM_{10} is below the national ambient air quality standard (NAAQS) of Thailand of 120 $\mu g\ m^{-3}$, then AQI $\leq$ 100 and a low (no) health risk is assigned to the area under consideration (Table S3). If 24 h PM_{10} is between 120 $\mu g\ m^{-3}$ and 350 $\mu g\ m^{-3}$, then the air quality is recognized as unhealthy. The PM levels in this range may cause effects to people in sensitive groups, i.e., with respiratory diseases (asthmatic people), old people, and children; hence, they should avoid prolonged outdoor activities. If 24 h PM_{10} is above 350 $\mu g\ m^{-3}$, then the air quality is recognized as very unhealthy and the general public should avoid outdoor activities.

The major difference in the risk scale between U.S. EPA and Thai PCD is in the AQI range from 100 to 200 for which U.S. EPA had two categories (unhealthy for sensitive groups: AQI of 101–150 and unhealthy for everyone with AQI: 151–200), while *PCD* [2017] has only one category (Table S3). Therefore, in this study, we use a modified scale of health risks by introducing a "moderate risk" with the concentration range of 121–254 $\mu g\ m^{-3}$, i.e., incorporating the Thai 24 h PM_{10} NAAQS (120 $\mu g\ m^{-3}$) as the lower limit and the U.S. EPA upper 24 h PM_{10} value of the unhealthy range (254 $\mu g\ m^{-3}$). Thus, the final risk scale used in our risk mapping for 24 h PM_{10} was (1) $<$120 $\mu g\ m^{-3}$: no/low risk; (2) 121–254 $\mu g\ m^{-3}$: moderate risk (unhealthy); and (3) $>$254 $\mu g\ m^{-3}$: high risk (very unhealthy). The AOT values corresponding to these 24 h PM_{10} cutoff values were first estimated using the regression model (improved with consideration of meteorological patterns), then mapping was done based on the AOT values that have a much better spatial coverage (than 24 h PM_{10} data in our domain). The detail of the risk scale for PM_{10} is presented later, in Table 2, along with the corresponding AOT regression results. To improve the spatial resolution of the MODIS AOT data, the spatial function, i.e., interpolation in Arcview GIS, was used to develop a continuous data set of AOT in the study domain during the haze prone period. For this interpolation, the inverse distance weighted method was used, which assumes that nearby data contribute more to the point being interpolated than data farther away [*Li and Heap*, 2008].

Table 1. Summary of PM_{10} Levels ($\mu g\ m^{-3}$) and AOT-PM_{10} Regression With and Without Consideration of Synoptic Patterns, February–April in Different Years

Parameters	Occurrence Frequency in February–April 2007	Period Average and Max 24 h PM_{10} (Brackets) at Four Stations[a], 2007	Period Average and Max 24 h PM_{10} (Brackets) at Two Chiangmai Stations[b], 2001–2008	AOT-PM_{10} Regression February–April 2007 (All Four Stations)
		Aver ± SD (Max)	Aver ± SD (Max)	Models With Statistics
Pattern 1	12%	43 ± 16 (93)	40 ± 15 (107)	$PM_{10} = -(14.8 \pm 55.4)$ AOT + (54.1 ± 26.2) $R^2 = 0.02$, $N = 6$, $p = 0.803$
Pattern 2	56%	137 ± 72 (396)	97 ± 54 (396)	$PM_{10} = (128.9 \pm 11.4)$ AOT + (39.4 ± 8.9) $R^2 = 0.51$, $N = 128$, $p < 0.0001$
Pattern 3	8%	102 ± 38 (188)	79 ± 41 (249)	$PM_{10} = (96.5 \pm 22.4)$ AOT + (37.5 ± 15.3) $R^2 = 0.51$, $N = 21$, $p = 0.0004$
Pattern 4	24%	128 ± 29 (353)[c]	89 ± 42 (236)	$PM_{10} = (107.4 \pm 26.4)$ AOT + (21.8 ± 28.7) $R^2 = 0.22$, $N = 59$, $p = 0.00014$
Combined (lump sum)	100%	121 ± 52 (396)	87 ± 45 (396)	$PM_{10} = (109.6 \pm 9.6)$ AOT + (41.4 ± 8.3) $R^2 = 0.37$, $N = 214$, $p < 0.0001$

[a]Data from Lampang station were not included due to the potential strong influence of industrial related emissions and cloudiness.
[b]Data from 2 Chiangmai stations only, as other stations were not operated before 2007.
[c]Maximum level was observed at the Mae Hong Son station.

The exposure mapping was done for the Chiangmai province, the largest and most populated province in the domain, as mentioned earlier. The layers of classified risk levels were overlaid over the Chiangmai province to map the risk that is considered together with the layer of population density. The obtained maps were analyzed with the wind data (windrose plots) to reveal the potential pollution transport from the upwind locations with intensive forest fires to the different parts of the province. The windrose plots in this study were generated by the Wind Rose Plots View™ software, which can be downloaded from http://www.weblakes.com, using the observed hourly wind data (speeds and directions) at the Chiangmai station provided by the Thailand Meteorological Department.

3. Results and Discussion

3.1. AOT and PM_{10} Regression

3.1.1. PM_{10} Levels

A summary of PM_{10} levels observed at four stations in Northern Thailand during the period of February–April 2007 is presented in Table 1, separately for different synoptic meteorological patterns and combined in the lump sum case for all patterns. In addition, the levels measured at two stations of Chiangmai during February–April of 8 years (2001–2008) are also presented separately for comparison. Other stations did not have data before 2007 for such a comparison. The monthly maximum 24 h PM_{10} of March (the highest daily level of the month) exceeded the Thailand NAAQS almost in 13 years during the 16 year period. The monthly maximum 24 h PM_{10} measured in Chiangmai (Figure 1) had the highest values in 2007 as compared to other years during the period of 2001–2016, as mentioned above; hence, March 2007 was selected for further risk mapping.

The results of the meteorological classification scheme presented in our previous study [*Kim Oanh and Leelasakultum*, 2011] showed that during the study period (February–April 2007), pattern 2 was observed most frequently, on 50 days (56%). Patterns 1, 3, and 4 were observed on 11 days (12%), 7 days (8%), and 21 days (24%), respectively (Table 1). The period average (3 months: February–April) PM_{10} levels were remarkably different between the synoptic patterns: pattern 2 had the highest levels followed by pattern 4. Pattern 1 had the lowest PM_{10} levels of all four patterns. The PM_{10} levels in different synoptic patterns in 2007 are consistent with the results for longer period (2001–2008) reported in the previous study [*Kim Oanh and Leelasakultum*, 2011] and also for 2001–2016 analyzed in this study (Figure 1). Note that both patterns (2 and 4) having higher PM_{10} were more prevalent during the February–April 2007; hence, the combined lump sum PM_{10} average (of all four patterns) during the 3 month period was also high, 121 ± 52 $\mu g\ m^{-3}$.

3.1.2. Regression Analysis Without Consideration of Synoptic Patterns

The MODIS AOT (validated against AERONET AOT) was used for the regression analysis with observed PM_{10}. First, simple linear regressions between 24 h PM_{10} and MODIS AOT (both Terra and Aqua) were analyzed for each of five PCD stations in the domain. The correlation coefficients (R, calculated as the square root of the

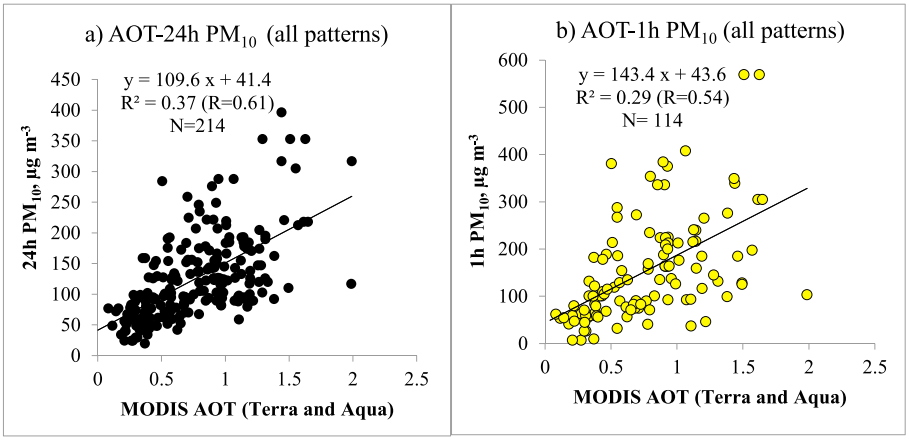

Figure 2. Scatter plots of MODIS AOT (Terra and Aqua) versus 24 h PM_{10} and 1 h PM_{10} (four ground stations), February–April 2007.

determination coefficient R^2) of AOT and 24 h PM_{10} measured at four stations of Chiangmai City Hall, Chiangmai Yupparaj, Chiangrai, and Mae Hong Son were 0.62, 0.66, 0.64, and 0.73, respectively. However, the correlation coefficient between satellite AOT and ground monitoring PM data in the Lampang station was quite low (R = 0.26). The presence of a large coal-fired power plant (Mae Moh, indicated in Figure S1) may be a reason for this poor correlation because the PM contributed by the stack gas emissions may induce a different AOT-PM relationship [*Mallet et al.*, 2003] than that for biomass burning smoke, the main influencing source in our study domain. A similar observation was also noted by *Sukitpaneenit and Kim Oanh* [2014], who analyzed the relationship between MODIS AOT and PM_{10} during the dry months of 2008–2010 for Northern Thailand. This further suggests that spatial parameters such as land use factors, e.g., location of point sources, road network, and others [*Liu et al.*, 2009], would be important to consider for improvement of the AOT-PM relationships. However, in our study domain, this power plant appears to be a single largest point source; hence, this factor cannot be directly included in the regression analysis. In addition, during the days of most heavy haze (10–15 March 2007), the cloudy sky (high cloudiness) was prevalent in Lampang, which affected the retrieval of MODIS AO; hence, the number of data points was small for an adequate regression analysis. Therefore, PM_{10} data of the Lampang station were not included in the further analysis of this study.

In the lump sum case, we used all daily (24 h) PM_{10} data measured at four stations (except Lampang) and MODIS AOT data (Terra and Aqua) available during the study period for the regression analysis, i.e., without segregating into the synoptic patterns. The results are summarized in Table 1, while Figure 2 presents a scatterplot showing an R^2 value of 0.37, i.e., a corresponding correlation coefficient (R) of 0.61 for this lump sum case. For comparison, the regression analysis between MODIS AOT and hourly PM_{10} (matching the satellite passing times: PM_{10} between10:00–11:00 A.M. for 10:30 A.M. of Terra and 13:00–14:00 for 13:30 Aqua passing time) is also presented. The regression model between AOT and 24 h PM_{10} is better than that between AOT and 1 h PM_{10} in terms of R^2 and with more data points (in many cases 1 h PM_{10} data were missing at the satellite passing time, while daily data could still be calculated using the observations at other hours of the day). For the exposure assessment purpose, as mentioned above, the 24 h PM_{10} data are also more relevant; hence, this study focused on 24 h PM_{10} for the purpose.

3.1.3. Regression Analysis With Consideration of Synoptic Patterns

The days of February–April 2007 were first separated into four homogeneous meteorological groups or synoptic patterns [*Kim Oanh and Leelasakultum*, 2011] with the occurrence frequency given in Table 1.

The MODIS AOT and 24 h PM_{10} relationships were analyzed for the days belonging to each pattern separately. The regression was done using all available PM_{10} data from four stations in Northern Thailand, and the resulting correlation coefficients between AOT and PM_{10} (square root of R^2 values given in Table 1) for patterns 2 and 3 were 0.71, respectively, that apparently higher than the lump sum case (R = 0.61). The regression for pattern 4 had a lower R (0.47) than the lump sum case, while pattern 1 (with only 6 data points) had a

poor correlation and even a negative slope. The standard deviation of the slope and intercept for each regression model are also presented in Table 1 along with the significance (p) of the linear regression produced by the analysis of variance. The significance (p) values showed that, except for pattern 1 ($p = 0.80$), all other cases presented in Table 1 show sufficient statistical evidence to conclude that there is a linear relationship between MODIS AOT and 24 h PM_{10} at significance level of <0.0005. Of a particular interest is the improvement of the regression model for pattern 2, which had a predominantly high occurrence frequency during the haze prone period. The improved model obtained for pattern 2 is specifically useful for the 24 h PM_{10} estimation using spatially more available MODIS AOT data in the domain.

The meteorological conditions of pattern 2, commonly featured a presence of a ground-based temperature inversion [*Kim Oanh and Leelasakultum*, 2011], had the lowest mixing height among the four patterns (330 m) and low wind speeds (Table S2), hence should enhance the pollution build up in the boundary layer. This pattern had the highest ground measured 24 h PM_{10} during the February–April 2007 period, i.e., with the maximum of 396 $\mu g\ m^{-3}$ (observed in Chiangmai) and an average PM_{10} over four northern stations of 137 $\mu g\ m^{-3}$ (Table 1). Because of its clear-sky conditions (lowest cloudiness of all four patterns: 1/10), pattern 2 had more AOT data points available for the regression analysis ($N = 128$; Table 1). The clear sky and low moisture content, i.e., the second lowest dew point of all four patterns, would reduce the bias of AOT values caused by cloud hygroscopic effects. A high R value for AOT-PM_{10} relationship found for pattern 2, together with its predominantly high occurrence frequency during the haze prone period (Table 1), had influenced the overall R value for the combined lump sum case. As a result, the R value for the lump sum case of 0.61, even without additional cloud screening (i.e., additional to the built-in cloud screening algorithm of MODIS AOT retrievals), was higher compared to other studies which reported R values of generally below 0.5 ([*Zeeshan and Kim Oanh*, 2014; *Dinoi et al.*, 2010] as seen in Table S1) found for the regression with PM_{10}. The higher R value found in our study as compared with *Zeeshan and Kim Oanh* [2014] for Bangkok may also be attributed to a more homogenous influence of biomass burning smoke in our study domain as compared to multiple urban emission sources of the Bangkok city.

The R value for pattern 3 also showed an improvement to 0.71 as compared to the lump sum case. This pattern had better dispersion conditions with the highest wind speed in Chiangmai (Table S2). In this pattern, the average PM_{10} over the February–April 2007 period and the maximum 24 h PM_{10} were 102 and 188 $\mu g\ m^{-3}$, respectively, which ranked third of all patterns (Table 1). The reason for the improvement of the R value in this pattern still needs to be analyzed together with the vertical profiles [*Zeeshan and Kim Oanh*, 2014] and the influencing emission sources of aerosol. Overall, the total number of data points available for the regression analysis for this pattern was still quite small ($N = 21$); hence, a longer study period is still required to produce more statistically inferred results.

Two patterns, pattern 1 and pattern 4, showed a reduction in R values as compared to the combined case. Pattern 1 had only a small number of data points available for the analysis ($N = 6$; Table 1) that made the regression result not statistically inferred, i.e., a negative slope with a high standard deviation (-14.8 ± 55.4) and a significance P value of 0.80 (showing a high probability of making error in inferring that there is a linear relationship between AOT and 24 h PM_{10}, well above a commonly used significance level of 0.05 in the environmental studies). This pattern occurred only on 11 days during the 3 month study period, and because of its overcast conditions, the built-in cloud screening algorithm of MODIS AOT retrievals removed the cloudy days, leaving only 6 days having MODIS AOT data. This pattern has the lowest PM levels during the study period with the average of 43 $\mu g\ m^{-3}$ and the maximum 24 h PM_{10} of 93 $\mu g\ m^{-3}$. The high mixing height (the highest in all patterns) and moderate wind speeds (1.1 $m\ s^{-1}$, the second highest) observed in this pattern would lead to a better dilution of PM emission (than pattern 2, for example). Thus, the high cloudiness observed in this pattern reduced the number of data points available for a more statistically inferred regression analysis. The cloudiness may also result in a certain bias of the predicted PM levels using AOT values [*Lee et al.*, 2011].

The R value for pattern 4 was 0.47, i.e., lower than the lump sum case (0.61). This pattern was quite similar to pattern 2 in terms of average meteorological conditions in Chiangmai but had different horizontal pressure gradients between Chiangmai and the regional stations. Pattern 4 mainly occurs in February, and it shows the influence of a strengthening high-pressure ridge over Northern Thailand [*Kim Oanh and Leelasakultum*, 2011]. The PM_{10} levels during the February–April 2007, averaged over four stations, were 128 $\mu g\ m^{-3}$, while the

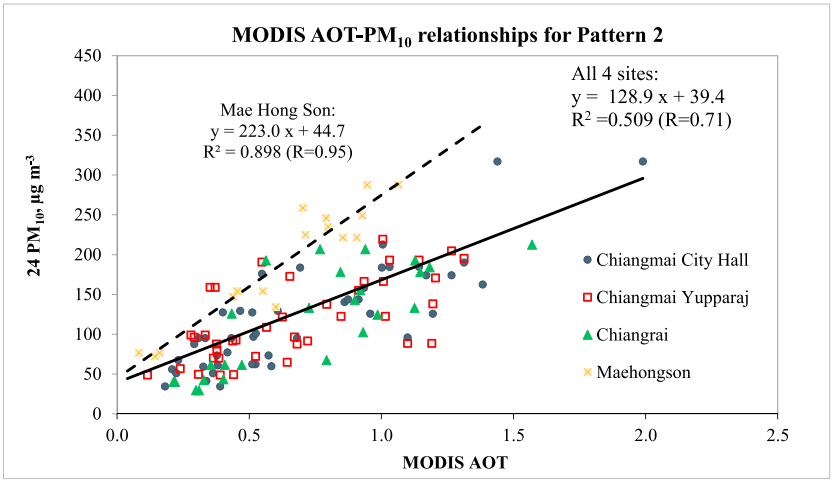

Figure 3. Scatter plot of MODIS AOT versus 24 h PM_{10} (four stations) for the days belonging to pattern 2, February–April 2007.

maximum 24 h PM_{10} was 353 µg m^{-3}, which was observed outside the Chiangmai province (at Mae Hong Son station; Figure S1). The total number of data points available for the regression analysis was moderate (N = 59). Pattern 4 was shown in our previous study [*Kim Oanh and Leelasakultum*, 2011] to feature a presence of a strong ground-based inversion that may cause an excessive amount of PM be trapped near the ground. Further studies should analyze the aerosol vertical profiles to provide a better explanation of the AOT-PM relationship in each pattern [*Zeeshan and Kim Oanh*, 2014].

3.2. Exposure Risk Mapping

As a case study to illustrate this approach, the exposure risk mapping was done for the Chiangmai province during the most severe haze period of February–April of 2007 from the entire 16 year period (2001–2016). The province is most populated and had the highest 24 h PM_{10} levels measured during the haze period in 2007. As mentioned above, pattern 2 occurred most frequently during the haze prone period and had the highest 24 h PM_{10} levels in Chiangmai; hence, the improvement in the AOT-PM regression for pattern 2 was specifically useful for the exposure risk mapping. The scatterplots of MODIS AOT versus PM_{10} measured at four stations in Northern Thailand for the days that belong to pattern 2 are shown in Figure 3. Station-wise, the R value was the highest (0.95) for the Mae Hong Son station, a rural background site, which had generally higher PM_{10} levels during the study period. This site may be more influenced by the forest fire smoke as shown by the large number of fire hot spots during the burning season [*Sukitpaneenit and Kim Oanh*, 2014]. The rest three stations, including two urban sites of Chiangmai and a rural background site of Chiangrai, had almost similar AOT-PM_{10} regression lines. The improvement of the regression model for Mae Hong Son station further suggests that the spatial predictors related to land use types should be considered in future studies for larger domains such as the entire Northern Thailand and neighboring countries. This study used the regression model developed for pattern 2 using data from all four stations, recognizing the fact that the Chiangmai province has different land use types (Figure S2); thus, a consideration of all stations (representing different land use types) would provide more representative results.

The regression model between MODIS AOT and 24 h PM_{10} (using PM_{10} data from all four stations) for pattern 2 was used to convert the PM_{10} concentration ranges specified in the modified exposure risk scales to the corresponding MODIS AOT ranges (Table 2). The mapping was then done using the MODIS AOT values, which were more available and spatially continuous, hence allowing the exposure risk identification in every part of the study area. The exposure risk categories were determined for every day of pattern 2 during the study period and were comparatively analyzed with the daily windroses. A summary of the areas (km^2) of the Chiangmai province that were identified under the three exposure risk categories is presented in Table 3 together with related parameters (wind and hot spot counts) for the days of pattern 2 in March 2007. Note that in this month, pattern 2 was identified on 26 days (out of 31 days). The 24 h PM_{10} levels in these

Table 2. Ranges of AOT Values Corresponding to 24 h PM_{10} in Low, Medium, and High Risk Levels

Scale No.	Category	24 h PM_{10} ($\mu g\ m^{-3}$)	AOT Upper and Lower Limits[a]
1	Low risk	0–120 (moderate)	0–0.625
2	Medium risk	121–254 (unhealthy)	0.626–1.665
3	High risk	>254 (very unhealthy)	>1.665

[a]AOT values were derived using the regression model for pattern 2 (Table 1).

26 days of pattern 2 observed in Chiangmai ranged between 77 and 396 $\mu g\ m^{-3}$. It is further noted that principally, the pattern classification should be done a priori and the regression equation for pattern 2 should be applied for the days belonging to this pattern only. However, the nearly absolute prevalence of pattern 2 in March of 2007, the month with highest PM_{10} in Chiangmai, suggests that the regression model obtained for pattern 2 can be generally used for PM_{10} estimation for the whole month of March.

The use of AOT values thus helped to get a spatially continuous interpolation of the exposure risk levels in the Chiangmai province for the exposure mapping purpose for every day. In fact, only 1 day (23 March) presented in Table 3 had a low exposure risk, while the rest 25 days of pattern 2 showed some areas of the province under at least the medium risk category. Four days had some areas, mainly urban parts, having been classified as under the high risk category, i.e., 10, 11, 12, and 13 March (bold in Table 3) with the area of the high exposure risk of 37, 47, 1053, and 1211 km^2, respectively. The most striking feature of these four days with the high exposure risk category was the high percentage of calm wind (50–88%) and very low average wind speeds, i.e., $<1\ m\ s^{-1}$ (Table 3). The wind directions varied widely in each day, mainly because of the low wind speeds. In fact, Chiangmai province has a large forest cover and the province is surrounded by forest areas of the neighboring provinces; therefore, winds of all directions can bring in the emissions from forest fires. The

Table 3. The Area of Different Risk Levels of Chiangmai Province and Related Factors for Days of Pattern 2 in March 2007

Date March, 2007	24 h PM_{10} in Chiangmai, $\mu g\ m^{-3}$	Risk Prone Area (km^2)			Daily Average Wind ($m\ s^{-1}$)	Calm Wind Frequency, %	Hot Spot Counts Within Radius 150 km of Chiangmai	Prevalent Wind Directions of the Day
		Low	Medium	High				
1	(173)[a]	15,486	4,855	0	0.4	79	80	NNE, ENE, ESE, S, SW
2	(176,191)	18,821	1,520	0	1.4	50	212	SW
3	(141,169)	18,061	2,280	0	0.9	54	122	E, W, SW
4	(184)	17,543	2,798	0	0.4	83	585	S
5	(240)	9,498	10,844	0	0.9	58	23	SSW
6	(213,219)	11,054	9,288	0	0.8	54	606	S
7	(127,159)	19,271	1,070	0	2.3	38	370	W
8	(150)	15,331	5,011	0	2.0	38	462	WSW
9	(129)	19,746	596	0	2.0	33	601	SW
10	**(190,195)**	**4,960**	**15,345**	**37**	**1.0**	**50**	**244**	WNW, WSW, SW, SE
11	**(234)**	**6,799**	**13,496**	**47**	**0.6**	**62**	**107**	NE, SSW
12	**(278)**	**1,618**	**17,670**	**1,053**	**0.5**	**75**	**18**	ENE, S, SSW
13	**(317,396)**	**8**	**19,122**	**1,211**	**0.2**	**88**	**464**	W, WSW
14	(260,287)	6,407	13,934	0	0.7	58	126	S
15	(174,205)	13,839	6,503	0	0.9	54	426	S
16	(162,171)	7,567	12,774	0	0.9	62	275	S
17	(182,197)	1,325	19,017	0	1.0	42	157	NNE, E
18	(185,193)	7,631	12,711	0	0.6	62	343	NE, E, SW
19	(174,175)	0	20,341	0	1.2	46	208	W, SW
23	(77,92)	20,341	0	0	1.3	46	172	SE, SSE, S, SSW, SW
24	(126,138)	4,044	16,297	0	1.3	42	308	SW
25	(158,166)	14,635	5,706	0	1.0	50	221	W
26	(140,138)	11,926	8,415	0	1.8	29	161	SSW
29	(122,122)	3,467	16,874	0	1.1	50	290	SSW
30	(93,88)	476	19,865	0	2.2	17	55	S, W
31	(96,88)	13,516	6,825	0	1.4	38	182	S, SSW

[a]Two stations in Chiangmai; only one value is presented if the other missing. The days with the high risk of exposure are bold.

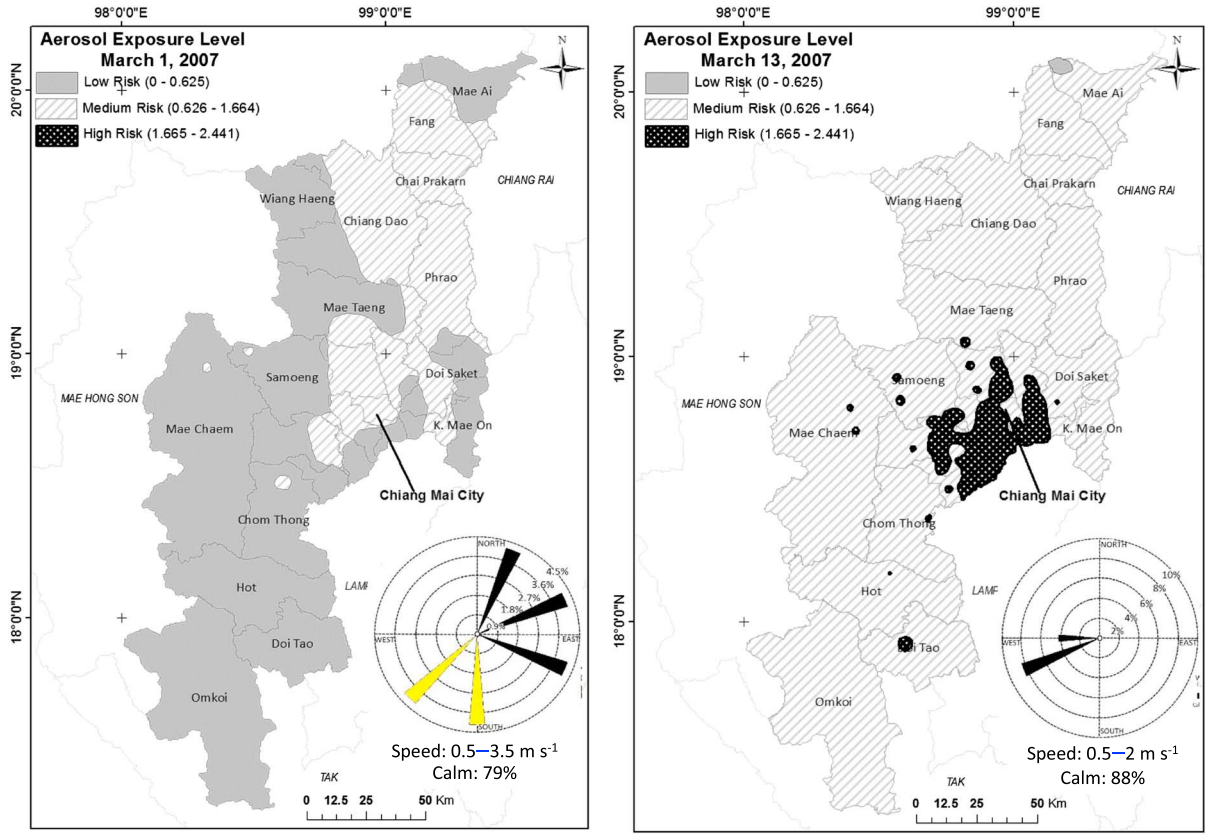

Figure 4. Exposure risk map to 24 h PM_{10} pollution for Chiangmai on 1 March (no high exposure risk) and 13 March 2007 (mostly medium and high exposure risk). The 24 h PM_{10} range for different risk categories: 0–120 μg m^{-3} for low risk; 121–254 μg m^{-3} for medium risk; and >254 μg m^{-3} for high risk.

hot spots can be used to present fires [*FIRMS Web Fire Mapper*, 2008], and this study used the hot spot counts within a circle of 150 km radius around the Chiangmai city, and the counts are also provided in Table 3.

The exposure map for 13 March, the day with the maximum 24 h PM_{10} and the largest area under the high exposure risk category specified for the Chiangmai province, is presented in Figure 4. 13 March had a large number of hot spots (464; Table 3) that were seen densely distributed in the study area (Figure S2), the calm wind percentage was the highest (88%), and the wind speed was very low (average of 0.2 m s^{-1}). These were the main reasons for the highest 24 h PM_{10} level measured in the province with the largest area under the high exposure risk category on the day. The large hot spot counts in fact were also recorded during the period of 6–9 March, but the wind speeds were higher with less calm wind (about 38%) that perhaps lowered PM_{10} levels. 1 March also had a large percentage of calm wind (79%) and low wind speed (0.4 m s^{-1}) but with a low hot spot count (80) and the low PM_{10} levels. The risk exposure map for 1 March 2007 is also presented in Figure 4 for comparison that showed that most the area of the province was categorized under the low-risk category (24 h $PM_{10} < 120$ μg m^{-3}), and the rest was under medium risk (24 h PM_{10}: 121–254 μg m^{-3}); i.e., no area was under the high exposure risk (24 h $PM_{10} > 254$ μg m^{-3}).

Thus, it appeared that the low wind speeds coupled with the large hot spot counts (forest fires) were important factors causing the high PM pollution during 10–13 March period. It is speculated that under the stagnant air conditions (calm wind), the emissions from forest fires would not be dispersed far from the burning locations, hence would remain in the area for several days, thus continued to contribute to high PM_{10} levels. On other hand, the areas with a high exposure risk were mainly observed in the urban parts of the province with a higher population density (a population density map is inserted in Figure S2), hence would cause more cases suffering from the exposure. In terms of emission sources this also suggested that the urban activities also contributed to the high pollution level in these stagnant air conditions. *Kim Oanh and Leelasakultum* [2011] reported that the seasonal industries may also be an important emission source

contributing to high pollution during the haze episode in March 2007, along with the major contributor of biomass open burning (forest and agricultural fires).

4. Conclusions

The application of the satellite MODIS AOT data could help to overcome the limitation in the spatial coverage of ground monitoring PM_{10} data for the exposure assessment purpose. The MODIS AOT-PM_{10} relationships are affected by the synoptic meteorological patterns that represent the totality of the meteorology governing over the study area. The consideration of synoptic patterns had improved the MODIS AOT-PM_{10} regression model for synoptic pattern 2, which was the most prevalent during the haze prone period of February–April in Northern Thailand. The correlation coefficient (0.71) between MODIS AOT and 24 h PM_{10} for pattern 2 was higher than the lump sum case (for all synoptic patterns), and the linear regression is statistically significant.

The improved MODIS AOT-PM_{10} regression model of pattern 2 was used to convert the corresponding 24 h PM_{10} concentration ranges of three risk categories to the MODIS AOT values that were subsequently used for the exposure risk mapping. The exposure map for Chiangmai, the largest and most populated province in Northern Thailand during the most severe haze month of March 2007, showed that the more populated urban parts of the province were under the higher risk of exposure to PM_{10} pollution. Intensive forest fires in the study area, indicated by a large number of hot spot counts, and the calm wind conditions were important factors leading to the high PM pollution levels, hence the high exposure risk in the province during the haze prone period. Future studies should cover a longer study period (more years) and should analyze the vertical aerosol profiles to better explain the improvement of MODIS AOT and PM_{10} relationships in given synoptic patterns. Spatial factors of land cover and land use types (forest area, urban area, road network, locations of point sources, etc.) should be considered to further improve the regression models between AOT and PM when a larger domain such as the Northern Thailand and neighboring areas is considered.

A concrete plan for public health care with early warning systems should be developed to reduce exposure of local people during haze episodes. More strict emission controls for all sources should be applied in March month when a high occurrence frequency of the stagnant air pattern (pattern 2: hot weather and calm wind) and more potential of forest fires are expected in Northern Thailand and surrounding territories.

Acknowledgments

All data used in the analysis are listed in the references and in the supporting information. Specifically, the authors would like to thank the Pollution Control Department of Thailand for providing the ambient air monitoring data, the Thai Meteorology Department for meteorological data, and the Goddard Space Flight Center Data for MODIS data. Appreciation is also extended to the FIRMS Web Fire Mapper for providing the hot spot data online. We would like to thank Muhammad Zeeshan from the National University of Sciences and Technology, Islamabad, Pakistan, for his assistance in interpreting the AERONET AOT data for comparison with MODIS AOT. The great assistance of Dang Anh Nguyet and Didin Permadi Agustian, from the air quality research group at AIT, in revising figures is specifically acknowledged.

References

Abou-Khadra, M. K. (2013), Association between PM_{10} exposure and sleep of Egyptian school children, *Sleep Breath.*, *17*(2), 653–657.

Brunekreef, B., and B. Forsberg (2005), Epidemiological evidence of effects of coarse airborne particles on health, *Eur. Respir. J.*, *26*(2), 309–318.

Chiangmai Provincial Public Health Office (CMPHO) (2008), http://www.chiangmaihealth.com, (accessed November 2015).

Chudnovsky, A. A., P. Koutrakis, I. Kloog, S. Melly, F. Nordio, A. Lyapustin, Y. Wang, and J. Schwartz (2014), Fine particulate matter predictions using high resolution aerosol optical depth (AOD) retrievals, *Atmos. Environ.*, *89*, 189–198.

Co, H. X., N. T. Dung, N. T. Kim Oanh, N. T. Hang, N. H. Phuc, and H. A. Le (2014), Levels and composition of ambient particulate matter at a mountainous rural site in Northern Vietnam, *Aerosol Air Qual. Res.*, *14*, 1917–1928.

Dinoi, A., M. R. Perrone, and P. Burlizzi (2010), Application of MODIS products for air quality studies over southeastern Italy, *Remote Sens. (Basel)*, *2*(7), 1767–1796.

Engel-Cox, J. A., C. H. Holloman, B. W. Coutant, and R. M. Hoff (2004), Qualitative and quantitative evaluation of MODIS satellite sensor data for regional and urban scale air quality, *Atmos. Environ.*, *38*, 2495–2509.

Engel-Cox, J. A., R. M. Hoff, R. Rogers, F. Dimmick, A. C. Rush, J. J. Szykman, J. Al-Saadi, D. A. Chu, and E. R. Zell (2006), Integrating lidar and satellite optical depth with ambient monitoring for 3-dimensional particulate characterization, *Atmos. Environ.*, *40*, 8056–8067.

Engel-Cox, J. A., N. T. Kim Oanh, A. Van Donkelaar, R. V. Martin, and E. Zell (2013), Toward the next generation of air quality monitoring: Particulate matter, *Atmos. Environ.*, *80*, 584–590.

Fann, N., A. D. Lamson, S. C. Anenberg, K. Wesson, D. Risley, and B. J. Hubbell (2012), Estimating the national public health burden associated with exposure to ambient $PM_{2.5}$ and ozone, *Risk Anal.*, *32*(1), 81–95.

FIRMS Web Fire Mapper (2008), https://firms.modaps.eosdis.nasa.gov, (accessed 15 May 2012).

Forest Fire Control Division (2011), http://www.dnp.go.th/forestfire/2546/firestatistic%20Th.htm, (accessed 15 August 2015).

Guo, J., X. Zhang, C. Cao, H. Che, H. Liu, P. Gupta, H. Zhang, M. Xu, and X. Li (2010), Monitoring haze episodes over the yellow sea by combining multisensor measurements, *Int. J. Remote Sens.*, *31*, 4744–4755.

Gupta, P., and S. A. Christopher (2008), Seven year particulate matter air quality assessment from surface and satellite measurements, *Atmos. Chem. Phys.*, *8*, 3311–3324.

Hopke, P., et al. (2008), Urban air quality in the Asian region, *Sci. Total Environ.*, *404*, 103–112.

Hyer, E. J., J. S. Reid, and J. Zhang (2011), An over-land aerosol optical depth data set for data assimilation by filtering, correction, and aggregation of MODIS collection 5 optical depth retrievals, *Atmos. Meas. Tech.*, *4*, 379–408.

Kim Oanh, N. T., and K. Leelasakultum (2011), Analysis of meteorology and emission in haze episode prevalence over mountain-bounded region for early warning, *Sci. Total Environ.*, *409*, 2261–2271.

Kim Oanh, N. T., et al. (2006), Particulate air pollution in six Asian cities: Spatial and temporal distributions, and associated sources, *Atmos. Environ.*, *40*, 3367–3380.
Kim Oanh, N. T., L. B. Thuy, D. Tipayarom, B. R. Manadhar, P. Pongkiatkul, C. D. Simpson, and L.-J. Liu Sally (2010), Source characterization of aerosol emission from field burning of rice straw, *Atmos. Environ.*, *45*(2), 493–502.
Kim Oanh, N. T., P. Didin Agustian, N. H. Phuc, and Y. H. Zhuang (2012), Chapter 1: Current status of air quality and management practices in Asian developing countries, in "*Integrated Air Quality Management: Asian Case Studies*", edited by N. T. Kim Oanh, pp. 1–60, CRC Press, Taylor and Francis, Boca Raton, Fla.
Kim Oanh, N. T., N. Thanh Hang, T. Aungsiri, T. Worrarat, and T. Danutawat (2016), Characterization of particulate matter measured at remote forest site in relation to local and distant contributing sources, Aerosol Air Qual. *Res.*, *16*, 2671–2684, doi:10.4209/aaqr.2015.12.0677.
Lee, H. J., Y. Liu, B. A. Coull, J. Schwartz, and P. Koutrakis (2011), A novel calibration approach of MODIS AOD data to predict $PM_{2.5}$ concentrations, *Atmos. Chem. Phys.*, *11*, 7991–8002.
Li, J., and A. D. Heap (2008), A review of spatial interpolation methods for environmental scientists, Geoscience Australia, Record, 2008/23.
Li, L., J. Yang, and Y. Wang (2015), Retrieval of high-resolution atmospheric particulate matter concentrations from satellite-based aerosol optical thickness over the Pearl River Delta Area, China, *Remote Sens. (Basel)*, *2015*(7), 7914–7937.
Liu, Y., J. Sarnat, V. Kilaru, D. Jacob, and P. Koutrakis (2005), Estimating ground-level $PM_{2.5}$ in the eastern United States using satellite remote sensing, *Environ. Sci. Technol.*, *39*, 3269–3278.
Liu, Y., M. Franklin, R. Kahn, and P. Koutrakis (2007), Using aerosol optical thickness to predict ground-level $PM_{2.5}$ concentrations in the St. Louis area: A comparison between MISR and MODIS, *Remote Sens. Environ.*, *107*, 33–44.
Liu, Y., C. J. Paciorek, and P. Koutrakis (2009), Estimating regional spatial and temporal variability of $PM_{2.5}$ concentrations using satellite data, meteorology, and land use information, *Environ. Health Perspect.*, *117*, 886–892.
Mallet, M., J. C. Roger, S. Despiau, O. Dubovik, and J. P. Putaud (2003), Microphysical and optical properties of aerosol particles in urban zone during ESCOMPTE, *Atmos. Res.*, *69*, 73–97.
Malm, W. C., D. E. Day, and S. M. Kreidenweis (2000), Light scattering characteristics of aerosols as a function of relative humidity: Part I—A comparison of measured scattering and aerosol concentrations using the theoretical models, *J. Air Waste Manag. Assoc.*, *50*, 686–700.
National Statistical Office of Thailand (NSO) (2016), Thailand-Population and Housing Census 2010. [Available at http://www.ilo.org/surveydata/index.php/catalog/1127/accesspolicy. (Accessed Jan 2017).]
O'Neill, N. T., T. F. Eck, A. Smirnov, B. N. Holben, and S. Thulasiraman (2003), Spectral discrimination of coarse and fine mode optical depth, *J. Geophys. Res.*, *108*(D17), 4559, doi:10.1029/2002JD002975.
Ostro, B., L. Chestnut, N. Vichit-Vadakan, and A. Laixuthai (1999), The impact of particulate matter on daily mortality in Bangkok, Thailand, *J. Air Waste Manag. Assoc.*, *49*, 100–107.
Park, H. Y., S. Bae, and Y. Hong (2013), PM_{10} exposure and non-accidental mortality in Asian populations: A meta-analysis of time-series and case-crossover studies, *J. Prev. Med. Public Health*, *46*(1), 10–18.
Pollution Control Department (PCD) (2017), http://www.pcd.go.th, (accessed March 2017).
Steinbach, M., G. Karypis, and V. Kumar (2000), A comparison of document clustering techniques, Proc. Workshop on Text Mining, 6th ACM SIGKDD Int. Conf. on Knowledge Discover and Data Mining.
Sohrabinia, M., and A. M. Khorshiddoust (2007), Application of satellite data and GIS in studying air pollutants in Tehran, *Habitat Int.*, *31*, 268–275.
Sukitpaneenit, M., and N. T. Kim Oanh (2014), Satellite monitoring for carbon monoxide and particulate matter during forest fire episodes in Northern Thailand, *Environ. Monit. Assess.*, *186*, 2495–2504.
Sapkota, A., A. P. Chelikowsky, K. E. Nachman, A. J. Cohen, and B. Ritz (2012), Exposure to particulate matter and adverse birth outcomes: A comprehensive review and meta-analysis, *Air Qual. Atmos. Health*, *5*(4), 369–381.
Song, C., C. Ho, R. J. Park, Y. Choi, J. Kim, D. Gong, and Y. Lee (2009), Spatial and seasonal variations of surface PM_{10} concentration and MODIS aerosol optical depth over china, *Asia-Pac. J. Atmos. Sci.*, *45*(1), 33–43.
Tillett, T. (2012), Hearts over time: Cardiovascular mortality risk linked to long-term PM2.5 exposure, *Environ. Health Perspect.*, *120*(5), a205.
Tsai, T., Y. Jeng, D. A. Chu, J. Chen, and S. Chang (2011), Analysis of the relationship between MODIS aerosol optical depth and particulate matter from 2006 to 2008, *Atmos. Environ.*, *45*(27), 4777–4788.
United Nation Environment Program-World Meteorological Organization (2011), *Integrated Assessment of Black Carbon and Tropospheric Ozone*, 249 pp., UNON/Publishing Services Section, Nairobi.
van Donkelaar, A., R. V. Martin, M. Brauer, N. C. Hsu, R. A. Kahn, R. C. Levy, A. Lyapustin, A. M. Sayer, and D. M. Winker (2016), Global estimates of fine particulate matter using a combined geophysical-statistical method with information from satellites, models, and monitors, *Environ. Sci. Technol.*, *50*(7), 3762–3772, doi:10.1021/acs.est.5b05833.
Wang, J., and S. A. Christopher (2003), Intercomparison between satellite-derived aerosol optical thickness and $PM_{2.5}$ mass: Implications for air quality studies, *Geophys. Res. Lett.*, *30*(21), 2095, doi:10.1029/2003GL018174.
Watson, J. G., and J. C. Chow (2002), Review of $PM_{2.5}$ and PM_{10} apportionment for fossil fuel combustion and other sources by the chemical mass balance receptor model, *Energy Fuel*, *16*(2), 222–260.
Weuve, J., R. C. Puett, J. Schwartz, J. D. Yanosky, F. Laden, and F. Grodstein (2012), Exposure to particulate air pollution and cognitive decline in older women, *Arch. Intern. Med.*, *172*(3), 219–227.
World Health Organization (WHO) (2003), Health aspects of air pollution with particulate matter, ozone and nitrogen dioxide, Bonn, Germany 2003. [Available at http://www.euro.who.int/__data/assets/pdf_file/0005/112199/E79097.pdf, (Accessed February 2016).]
World Health Organization (WHO) (2014), Air pollution estimates, 2014. [Available at http://www.who.int/mediacentre/news/releases/2014/air-pollution/en/, (Accessed 20 February 2016).]
Yahi, H., B. Marticorena, S. Thiria, B. Chatenet, C. Schmechtig, J. L. Rajot, and M. Crepon (2013), Statistical relationship between surface PM10 concentration and aerosol optical depth over the Sahel as a function of weather type, using neural network methodology, *J. Geophys. Res. Atmos.*, *118*, 13,265–13,281.
Yap, X. Q., and M. Hashim (2013), A robust calibration approach for PM_{10} prediction from MODIS aerosol optical depth, *Atmos. Chem. Phys.*, *13*, 3517–3526.
Zhang, H., R. M. Hoff, and J. A. Engel-Cox (2009), The relation between moderate resolution imaging spectroradiometer (MODIS) aerosol optical depth and $PM_{2.5}$ over the United States: A geographical comparison by U.S. environmental protection agency regions, *J. Air Waste Manage.*, *59*(11), 1358–1369.
Zeeshan, M., and N. T. Kim Oanh (2014), Assessment of the relationship between satellite AOD and ground PM_{10} measurement data considering synoptic meteorological patterns and lidar data, *Sci. Total Environ.*, *473–474*, 609–618.

Zheng, J., W. Che, Z. Zheng, L. Chen, and L. Zhong (2013), Analysis of spatial and temporal variability of PM_{10} concentrations using MODIS aerosol optical thickness in the Pearl River Delta Region, China, *Aerosol Air Qual. Res.*, *13*, 862–876.

Zhou, B., B. Zhao, X. Guo, R. Chen, and H. Kan (2013), Investigating the geographical heterogeneity in PM_{10}-mortality associations in the China air pollution and health effects study (CAPES): A potential role of indoor exposure to PM_{10} of outdoor origin, *Atmos. Environ.*, *75*, 217–223.